



# Structural Health Monitoring of Composite Aircraft Structures Using Fiber Bragg Grating Sensors

*Nitesh Gupta, M.J. Augustin, Sakthi Sathya, Saransh Jain, S.R. Viswamurthy, Kotresh M. Gaddikeri and Ramesh Sundaram*

**Abstract** | Aircraft industry is continually striving towards reducing the acquisition, operation and maintenance costs. Usage of advanced composite materials in primary aircraft structures have resulted in significant weight savings owing to their higher specific strength and specific stiffness. Composite structures, in spite of their inherent advantages, are prone to various damages. To detect and repair various structural damages that can occur during the service life of the aircraft, a thorough inspection schedule is implemented through conventional visual and Non Destructive Evaluation methods. Such scheduled inspections lead to considerable increase in maintenance cost & down-time of the aircraft. An online structural health monitoring (SHM) system consisting of well-designed sensor networks incorporated in the structure along with necessary hardware and software can provide information about the structure, thereby leading to reporting of flaws or damages in real time. Such a system can provide inputs for condition based maintenance which can result in reduced maintenance cost. This paper presents the work carried out at CSIR-National Aerospace Laboratories towards developing a flight-worthy SHM system and its demonstration on an unmanned aerial vehicle (UAV). Sensor selection, characterization, instrumentation design, algorithm development towards damage detection & load estimation at lab level and implementation of the technology on a UAV are discussed in this paper.

**Keywords:** *Structural Health Monitoring (SHM), Damage, Debond, Fiber Bragg Grating (FBG), Artificial Neural Network (ANN)*

## 1 Introduction

Aircraft industry continually strives towards reducing acquisition, operation and maintenance cost. The usage of composite materials have resulted in significant weight savings and cost benefits. However, designers are still conservative as these materials are relatively new and hence their complete potential is yet to be exploited. Techniques and methods for assessing fatigue, delaminations, disbonds and damage tolerance characteristics of these advanced materials can assist in reducing conservatism built in current aircraft structural design leading to realization of slender airframe structures.<sup>1</sup> Maintenance,

Repair and Overhaul (MRO) contributes significantly towards the operational cost of an aircraft, which also constitute preventive maintenance activities and scrapping of expensive parts, due to the conservative approach, even if they satisfy the required strength characteristics.<sup>2</sup> The complex nature of damages in composite structures necessitates periodic checking, which is usually carried out through visual inspection and ultrasonic NDE. These methods are sometimes limited by the inaccessibility of interior parts which may leave damages unidentified. Any solution, which continuously monitors the status of the structure and informs the concerned personnel, can lead to

a timely and cost effective solution to this problem. In this regard, various aircraft industries and research labs are pursuing development of systems and methods for structural health monitoring of composite aircraft structures. Structural Health Monitoring (SHM) has been defined in the literature as the “acquisition, validation and analysis of technical data to facilitate life-cycle management decisions”.<sup>3</sup> The time domain data with further analysis can be used for the usage monitoring, damage diagnosis and also provide a prognosis i.e. for the evolution of damage, residual life, etc. By taking advantage of the SHM system in place, one could conceive of a new “SHM based design” approach that would result in lower weight, thus reducing operating costs. Moreover, SHM should be dovetailed with a larger Integrated Vehicle Health Management (IVHM) system, encompassing other aircraft components such as avionics and power plant systems. Consequently, due to its potentially profound influence on aircraft design, safety and economics, SHM has become an important and widely pursued area of research.<sup>4</sup> Development of a SHM system involves the integration of sensors into the structures, data acquisition from the sensors at the required rate, data transmission to the data processing system, processing the data with the algorithm for extracting different features leading to usage monitoring, damage diagnosis and prognosis. The development Life-Cycle of a typical SHM system for aircraft application is shown in Figure 1.

Various sensor technologies and methodologies are being described in the literature for the development of a real time SHM system for aircraft application.<sup>4-7</sup> Sensor embedment methods and connectorisation schemes which will provide ease of operation and ensure safety of the sensors during production and service life of the aircraft

without hindering the production and assembly process are being developed. Deployment of multiple sensor types across the structure and acquisition of the sensor data with dedicated on-board instrumentation which is distributed in space, computer across the aircraft but communicating with central processing is the current trend which SHM community is trying to achieve.<sup>8</sup> On-board sensor measurement is instrument specific and must cater to the operating environment within the aircraft. As the data rate is very high and recording can go for long durations depending on the flight, enabling the different data acquisition nodes with some level of processing capability where the required features from the sensors are extracted and send to Central Processing Computer (CPC), will be one of efficient ways of utilizing the resources. Implementation of various validated algorithms in optimized codes at various subsystems along with data acquisition systems for load and damage monitoring will be the most challenging part in the SHM system development. A recent survey among various Aircraft OEMs and operators shows that delaminations, disbonds and impact induced damages continue to be perceived as significant threats to operational safety.<sup>9</sup> Accidental foreign body impact can create subsurface damages that can significantly reduce the strength and stiffness of a component. Necessary warning systems to notify the pilot or maintenance personnel about damages and load exceedances in real time, is the ultimate goal of SHM. Cumulative data recording over longer duration can serve as a data base for prognostics and SHM based design. Various SHM subsystems and their interaction are explained in detail by Balageas.<sup>10</sup>

The SHM group in the Advanced Composites Division, CSIR-NAL has been pursuing the development of an aircraft structural health monitoring

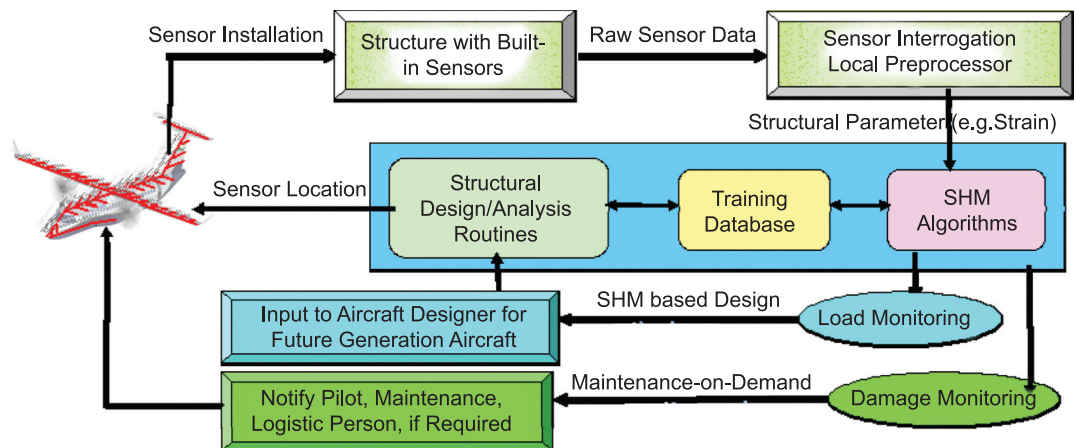


**Figure 1:** Life cycle of SHM system.

system that attempts to address the following (a) Sensor selection, characterization & their integration with primary aircraft structures (b) SHM instrumentation development for ground and flight tests (c) SHM methodology development (d) Flight trials with the on-board SHM system and (e) Development of SHM data processing algorithms and software. This paper focuses on the development of a flight-worthy SHM system for aircraft composite structures and its subsequent implementation on an unmanned aircraft.

## 2 Sensor Selection and Embedment

The majority of the SHM systems rely on the strain as measured parameters and through various algorithms the required damage information is extracted. A robust SHM framework requires the installation of a distributed sensor network so that damage measurements can be made quickly and frequently without significant effort or expense. Sensor technology has matured enough to have highly sensitive, reliable and miniaturized strain sensors which can be embedded or surface bonded to the composite structure during/after the manufacturing. Several types of sensor networks are being investigated, including strains<sup>11</sup> Piezo transducers<sup>12</sup> and fiber optic sensors.<sup>13</sup> Using these sensors, active and passive detection techniques have been proposed with some degree of success in metallic structures.<sup>14</sup> In passive detection, transducers are used to monitor perturbations directly caused by damage causing event (e.g. rapid release of acoustics energy or heat) or to record/monitor

structural responses (e.g. ambient vibration, loads, impact events). Acoustic Emission (AE) is the best known example of a passive technique used for damage detection in metallic structures. Passive approaches often require various mapping techniques to obtain information about usage or possible structural damage from signal responses. Lamb waves are also considered to be one of the ways to characterize the damage which requires actuation and sensing.<sup>15</sup> PZT based SMART<sup>®</sup> layers<sup>16</sup> PZT based Wireless impact and damage detection system by Metis design Corporation<sup>1</sup> are reported for active damage detection. Three-dimensional (3-D) laser Vibrometer<sup>17</sup> is another method for the estimation of the induced damage.

The advancement of fiber optic sensors has opened up some good choices for the SHM of Composite Structural Health monitoring. Fiber Optic (FO) sensors have several advantages such as low weight, high sensitivity, immunity to Electromagnetic Interference (EMI), multiplexing capability, etc. Fiber Optic sensors are of many types: Michelson Interferometer, Mach Zehnder Interferometer, Fabry-Perot Interferometer, and Fiber Bragg Grating (FBG) sensors.<sup>18–21</sup> Among the various FO sensors, Fiber Bragg Grating Sensors are considered to be the most preferred<sup>22</sup> for the aerospace application due to its durability under extreme environmental conditions, capability of dense multiplexing and ease of handling. The majority of the work presented in the paper is based on the FBG sensor. It relies on the narrow-band reflection from a region having a periodic

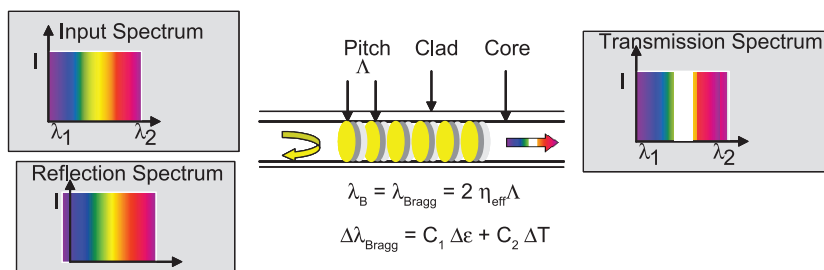


**Figure 2:** Fiber Bragg Grating schematic & working principle.

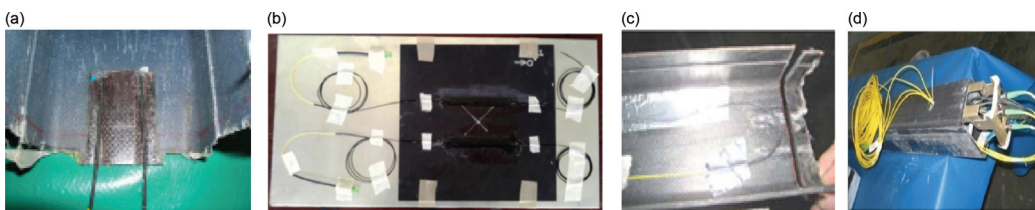


**Figure 3:** Sensor patch embedment (a) with embedment during fabrication (b) after fabrication (c) embedded structure during the trimming (d) after assembly.

variation in the core refractive index as shown in Figure 2. The shift in the reflected wavelength from the central wavelength of the FBG gives a direct measure of external perturbation in terms of strain or temperature. Reliable embedment is the proper handling of the egress points, where the fibers tend to break at the exit point of the composite structure due to the accumulation of small quantities of resin, which is very brittle & sharp. Various embedment studies have been conducted by use of Neoprene rubber or Teflon sleeve at the exit point or patch embedment schemes to ease the long-term handling of these delicate sensors.

In case of Fiber exiting through one side of the structure, the use of rubber and Teflon tube is the easy option but in most of the practical cases this will not be the situation as parts will general have to be trimmed. In such cases, sensor patch embedment schemes during and after fabrication have been developed and demonstrated from coupon to aircraft level as shown in Figure 3. As the sensor exit is not through the end, various trimming and assembly process can be carried out without disturbing the fiber exit point. Spectrum based quality assurance methods have also been developed to ensure the sensor integrity after the embedment fabrication and assembly.

Various tests were carried out (Tensile, compression and ILSS tests) on specimens embedded with optical fibers to study how the embedment affects the mechanical properties was no degradation in the mechanical properties due to the embedded optical fiber.<sup>4</sup>

### 3 Sensor Characterization Studies

It is important to study the behavior of sensors in terms of response towards physical parameters, sensitivity, directional sensitivity, sensing range, nature of the signal acquired etc. towards damage causing events. This will eventually help in designing the appropriate sensor cell/network to detect/predict various damages in composite structure with minimum possible error. As FBGs are sensitive to external parameters which change the pitch and effective refractive index, characterization studies were carried out for strain and temperature. The strain and temperature sensitivities were found to be 1.23 pm/micro strain and 10.94 pm/Deg C as shown in Figure 4(a) and (c) respectively. The response of the FBG towards dynamic events was also carried out and is presented in Figure 4(b). In addition to this, cross sensitivity tests were also carried out to ensure that strain sensitivity is not a function of temperature Studies led to the conclusion that FBG sensors strain response is well in agreement with Resistive Strain Gauge (RSG) sensors.

Above characterization studies include FBG sensors from different vendors and different data acquisition systems and found to be matching well. These studies led to the confidence of developing SHM systems based on FBG. Additional characterization studies were also carried out based on the requirement to ensure the response of FBG after embedment in different structures, response towards various loadings and events leading towards damage which are described in subsequent sections. These studies helped in fine tuning the sensor parameters and instrumentation

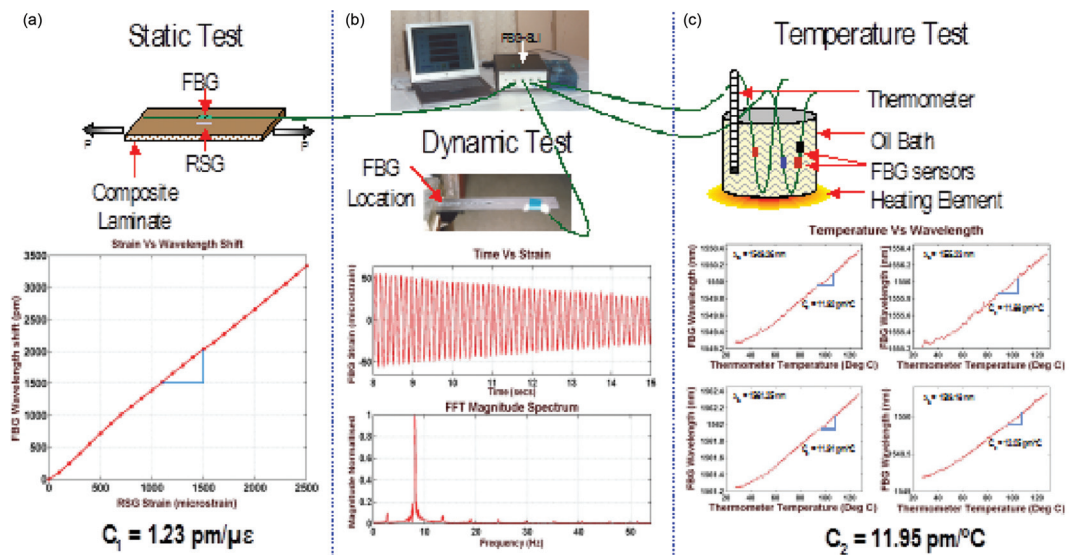


**Figure 4:** (a) Strain characterization (b) Response to dynamic event (c) Temperature characterization.



specification in terms of reflectivity, side lobe suppression etc. based on application.

**4 SHM Instrumentation**

Instrumentation development for the structural health monitoring system was carried out in two phases; for ground level applications and aircraft level application. Different commercial interrogation systems (Micron optics, Smart Fibers etc.) working on different operating principles are available in the market along with R&D outputs from academia and industry. Instrumentation schemes need to be designed and developed based on the parameters to be monitored and the nature of events causing the variation in the parameters. Micron optics- sm130 swept laser interrogator along with channel multiplexer were utilized for ground static tests and smart fibers Wx-M was used for dynamic and in-flight strain monitoring for the work described in this paper. NI PXIe 1062Q along with NI PXIe 4331 strain and NI PXIe 4472 dynamic data acquisition card based instrumentation systems is being used for RSG and other Voltage based data acquisition. Various data acquisition systems for lab level and flight level used in the study are shown in Figure 5.

Automation of the tests in terms of data acquisition, post processing and archiving is of utmost importance in the development of algorithms for SHM applications. For catering to the requirements, general purpose GUI based software’s for data acquisition, processing and archiving were developed with NI LabVIEW and DIAdem and are shown in Figure 6. Modular design approach has been implemented for ensuring the software scalability and reusability.

Scaling the ground based instrumentation to meet airworthiness requires fulfilling constraints based on the space, size, input power and operating environments. Ruggedized conectorisation and routing schemes need to be implemented to ensure the sensor data flow among various subsystems. Figure 7 shows one of the arrangements for self-powered data acquisition comprising of interrogator, battery bank, flight computer and necessary MIL connectors designed and integrated by the group. It has been conceived and developed for NISHANT UAV but can be modified easily for another flight requirement. This comprised of a solid state 4 channel FBG interrogator having a high acquisition rate (>2 KHz), on-board computer with solid state storage media, Lithium-Ion



**Figure 5:** Various data acquisition systems used in the SHM system development.

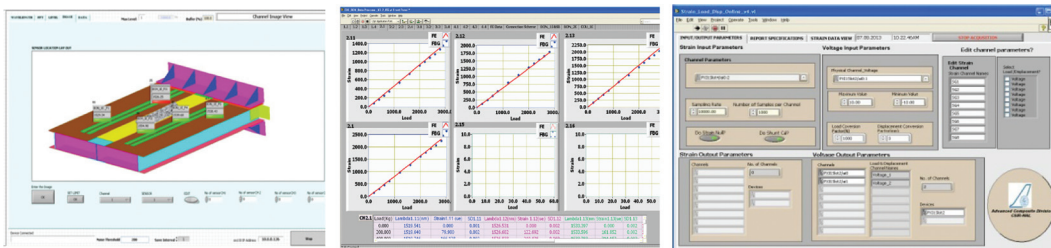


**Figure 6:** LabVIEW based GUI software for the data acquisition analysis and archiving for FBG and RSG data acquisition systems.

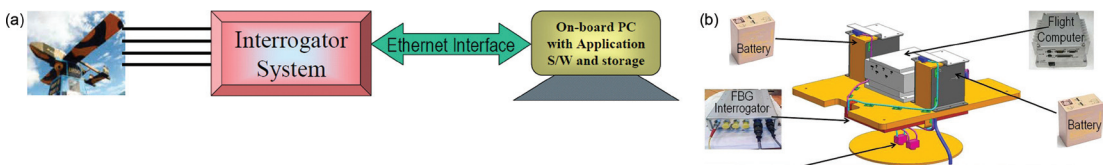


**Figure 7:** (a) Schematic of SHM instrumentation (b) Implementation for NISHANT UAV.

battery, electrical & fiber optic interconnects & mounting fixtures.<sup>23</sup>

## 5 SHM Methodology & Algorithm Development

Data collected from sensors (either of same type or different type) needs to be combined and interpreted for extracting the information about load and damage. This analysis includes the classification, location and severity of damage leading to a final prediction of remaining service life of the structure. In the absence of any damage information, the knowledge of flight operational load pattern will be useful for the designers in future designs. Processing of the large chunk of data and making sense out of it requires development of memory and time efficient software implementations. Sensor data coming to the data logger PC first get stored in it and passes through various algorithm subroutines utilizing the multiprocessing and multi-threading capabilities of modern computers. The basic assumption of most damage detection methods is that damage will alter the stiffness, mass or energy dissipation properties of a system, which in turn alter the measured dynamic and/or static responses of the system. However, the implementation of the detection scheme is challenging, due to a multitude of factors like local in nature and randomness of damage which requires an unsupervised learning mode along with difficulties in making accurate and repeatable response measurements from a limited number of locations on complex structures operating in adverse environments.

Different types of techniques which can be used for the development of SHM algorithms such as signal processing techniques, physics based modeling, fuzzy logic, genetic algorithms and Artificial Neural Networks (ANN). Most of the work carried out in the literature considers SHM as statistical pattern recognition problem,<sup>24</sup> which in general tries to extract out the feature sensitive to damage from sensor data. Forward and reverse problems based on natural frequency shifts, shift in model parameters based on Model Assurance Criterion (MAC),<sup>25</sup> use of the dynamic flexibility matrix,<sup>26</sup> response surface analysis<sup>27</sup> are some of the feature extraction methods which utilize the numerical model of the undamaged structure and experimental data for localizing and quantizing the damage. Many damage detection schemes utilize Artificial Neural Networks (ANN) to detect, localize, and quantify damage in structures<sup>28</sup> Optimization algorithms based on the genetic algorithms and simulated annealing are also being persuaded by various research groups.<sup>28</sup> Various

algorithms based on time of arrival/ time difference of arrival,<sup>29</sup> strain amplitude<sup>30</sup> have been proposed for the localization of damage based on active and passive sensing methods. Selection of the algorithm and its effective implementation for the specific application is one of the key steps in SHM methodology, as most of these algorithms are application/structure specific.

## 6 Development of SHM system and Methods—Lab Scale

Co-cured and co-bonded integrated construction of composite structures is leading to replacement of fasteners with bonded joints. In closed composite structures (box type), the rib/skin and spar/skin will be co-cured or co-bonded. In this type of construction, the weak link is the interface between the rib and skin or between the spar and skin. Various studies<sup>31,32</sup> led to the conclusion that among the different damage modes in co-cured and co-bonded composite structures, the critical area of concern is the skin-stiffener debond. In this construction technology, there could be process induced defects i.e. foreign inclusions, porosity, delaminations etc. From the structural health monitoring point of view it is imperative to detect the defects such as skin-stiffener debond in composite structures and assess the load acting in the presence or absence of these defects. Delaminations have been thought of as critical to structural integrity. It is known that the delaminations have practically little effect on the tensile strength, but the compressive strength is reduced. The residual strength in a laminate depends on the size and location of the delamination. Generally, low velocity impact which includes runway debris, tool drop and blunt impact from ground support equipment manifests itself as delamination's in a structure without leaving any visible/barely visible sign on the surface. SHM methodologies were developed to detect and quantize the damage along with load estimation at the lab level.

### 6.1 Debond and load estimation on composite test box

The above mentioned steps were used in the development of a system and method for detecting the debond has been developed and demonstrated on a test box structure. The details of the study and the results are presented in the following sections. In this study, a supervised learning paradigm was implemented based on Artificial Neural Networks. Implementation of ANN is a two-step process. In the first step, the network is trained using known input and output data. Once trained, the network can be used for prediction of a new input, which

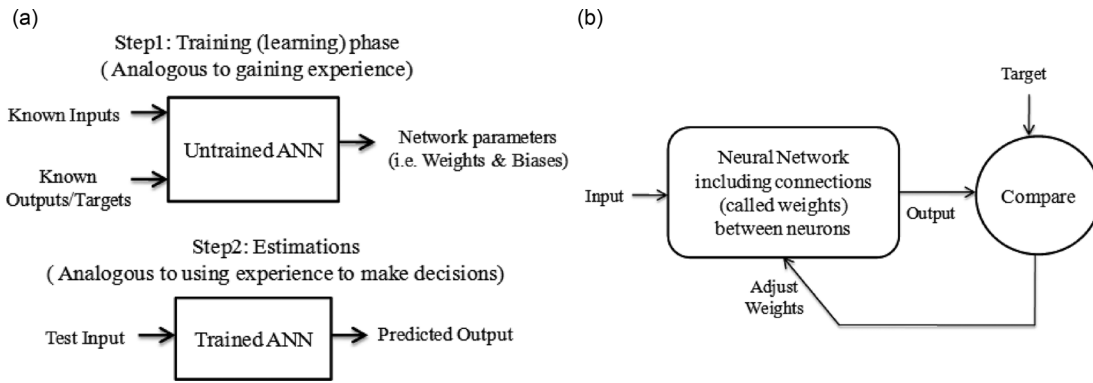


Figure 8: (a) The ANN principle (b) ANN training.

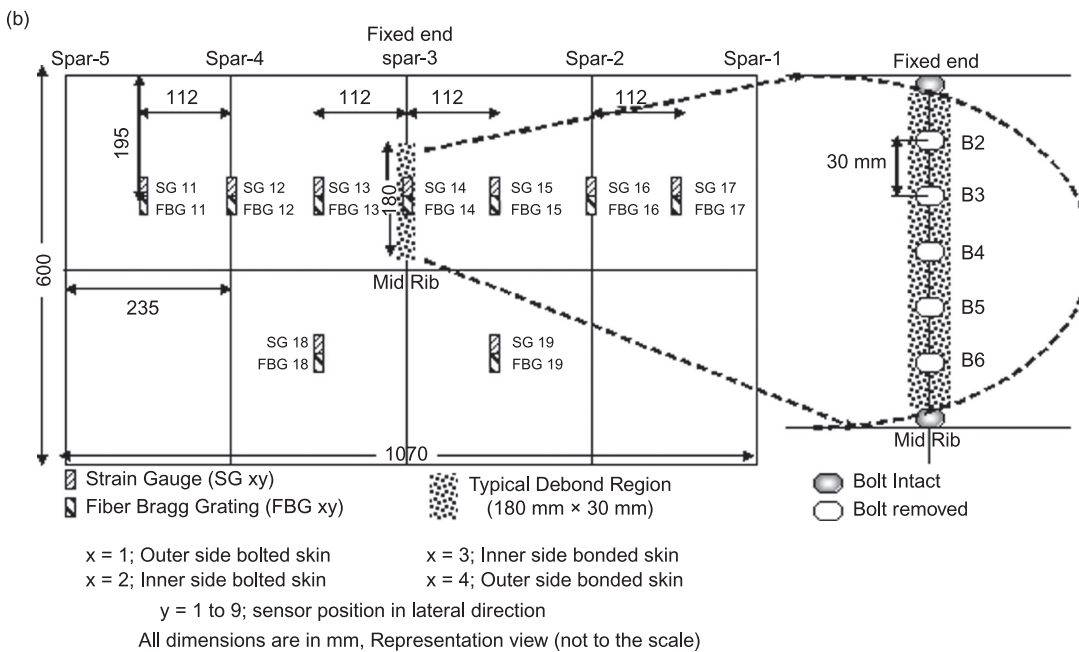
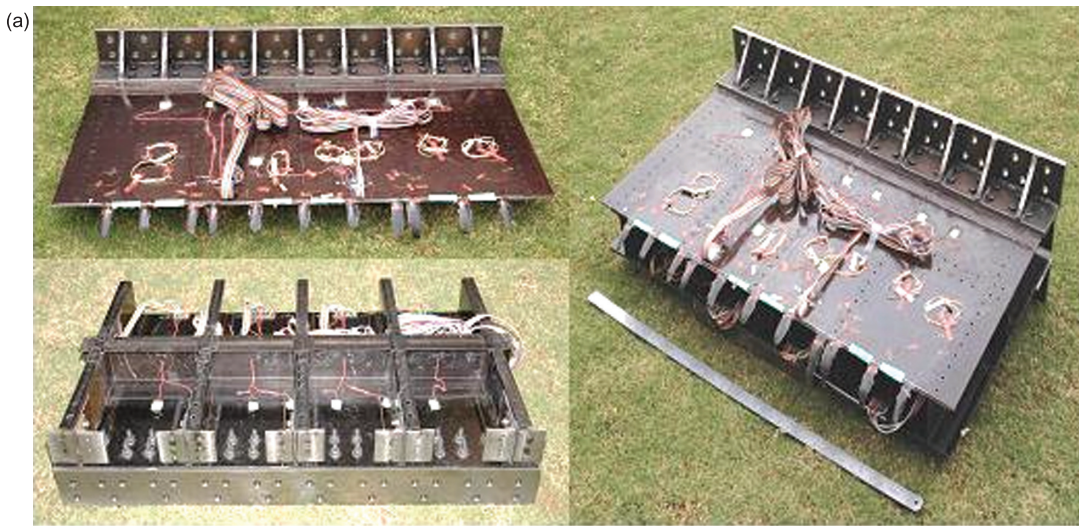


Figure 9: (a) Photograph (b) of sensor locations composite test box.

was not used for training (Figure 8(a)). Training involves adjusting the values of the connections (weights) between elements. Typically, neural networks are adjusted, or trained, so that a particular input leads to a specific target output. The training process is illustrated in Figure 8(b).

Studies were carried out on two composite test boxes and necessary algorithms were developed and validated. In the first box, controlled ‘debonds’ were created by selectively removing bolts.<sup>33</sup> The second box was fabricated with an intentionally created partial-span disbond between a spar and skin by placing non-adhesive inserts during lay-up. Tests were conducted and the disbond was progressively reduced in size by adhesively bonding the two parts.<sup>34</sup>

**6.1.1 Test box 1:** In order to address the issue of skin-stiffener debonds in composite structures, a multi-spar co-cured test box was fabricated using carbon/epoxy unidirectional prepreg tape (Hexcel T300/914C material system). The box comprised 5 spars, one central rib and two skins with dimensions 1070 × 600 × 155 (all in mm). The test box configuration is shown in Figure 9(a). Strain gauges and FBG sensors were fixed to the box. FBG sensors were embedded only in the top skin. Some FBGs were lost also surface bonded close to corresponding strain gauge. Figure 9(b) gives a sketch

showing the locations of the strain gauges and FBG sensors.

**6.1.1.1 Experimental studies:** The box was mounted in a cantilever condition using L-angles at one. The load was applied at the free end and was distributed equally at the five spar locations. Different healthy and unhealthy tests were carried out with the box. The healthy test kept all the bolts intact. This provided the baseline data with which the unhealthy cases were compared. The unhealthy cases were carried out by removing 5 bolts (B2 to B6, Refer Figure 9(b)) from the different spars from the root end. This was equivalent to a debond of size 180 mm × 30 mm. The possible unhealthy combinations were (i) Single spar unhealthy (bolts removed from one spar at a time), (ii) Two spars unhealthy (bolts removed from two spars simultaneously) and, (iii) Three spars unhealthy (bolts removed from all the three spars). Figure 10(a) shows the strain comparison away from the debond and on the debond for healthy and single spar-3 unhealthy case. Figure 10(b) (Right) shows the FBG measurement for the same case. It was found experimentally that the strain gets affected only in the close vicinity of the debond location. The strain pattern does not change significantly away from the debond. Figure 11 shows the percentage of  $\Delta\epsilon$  with respect

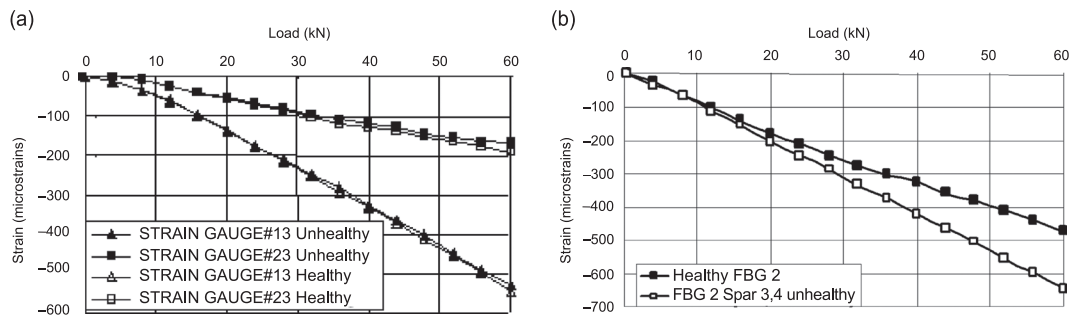


**Figure 10:** (a) Strain comparison away from the debond and on the debond for healthy and single spar-3 unhealthy case. (b) FBG measurement for the same case.

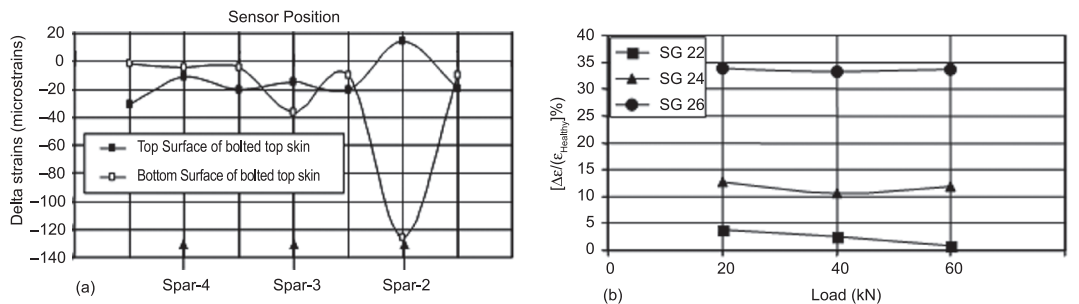


**Figure 11:** (a) Lateral variation in  $\Delta\epsilon$ , (b) percentage of  $\Delta\epsilon$  w.r.t. healthy strains for spar-2 unhealthy case.



to the healthy strains for the sensors on the inner side of bolted top skin at the spar location for different load cases for single spar (Spar-2) unhealthy case.

**6.1.1.2 SHM methodology & algorithms:** In order to develop the SHM methodology, two different sets of unhealthy cases were carried out on the test box (i) Fixed debond size on different spars and (ii) different debond size on one spar at a time. First case simulated the debond of fixed size (180 mm × 30 mm) on different spars. In the second case, the number of bolts removed at a time from single spar varied from 2 to 5 which simulated the debonds of lengths 60 to 180 mm (width = 30 mm).

Damage estimator developed for the first case was used to identify the damaged spar(s) and size. Damage estimator developed for the second case was used to identify the different damage sizes. In addition to this, a load estimator to predict the load acting on the structure was also developed. A novel sensor-grid approach was devised for the efficient working of these estimators. This was in accordance with the experimental observation that skin-stiffener debond is a local strain change phenomenon and strain will be affected only in the close vicinity of debond.

Above estimators were developed using feed forward back propagation based ANN. The experimentally validated FE strain values with corresponding damage size and load values were used for training the network. The performance evaluation of the network was carried out with the experimental data. Table 1 shows the results as

predicted by ANNs for fixed debond size on multiple spar at a time.

As in case of varying debond size on one spar at a time, there could be many combinations of same debond size for different bolt removal case along one spar (e.g. B2 and B3 bolt removal case will yield the same debond size as for B4 and B5 as shown in Figure 12), debond center from the fixed end was chosen as the target parameter to identify the exact location of damage on the spar. Here also three ANN approaches along with sensor-grid was adapted. Table 2 shows the prediction performance of the ANNs for this case.

It can be seen that the ANN's with the sensor—grid scheme were capable of identifying the damage location and size fairly well.

The objective of the load estimator was to predict the applied load based on the observed strain pattern. It is to be noted that training was done only with healthy strains. Performance evaluation of the network was conducted by applying the experimental strains to the network for known load and checking the predicted value of the load from the network. The experimental strains used to test the network include both healthy and unhealthy strains, although the network was trained only using healthy strains.

From Tables 3 and 4 it can be observed that the load estimation works best for healthy conditions and progressively deviates from the applied load as the degree of damage increases. This is to be expected since the strains, which form the inputs to the network are affected by the damage. Nevertheless, the estimation error does not exceed 13% in all the cases studied.

**Table 1:** Prediction performance of damage estimator for fixed debond size on multiple spars at a time.

Cases	Healthy			Single spar unhealthy (Spar 3)			Two spars unhealthy (Spar 2 & 3)			Three spars unhealthy (Spars 2, 3 & 4)		
	N2	N3	N4	N2	N3	N4	N2	N3	N4	N2	N3	N4
Target	0	0	0	0	5	0	5	5	0	5	5	5
Prediction	0	0	0	0	4.7	0	5	4.8	0	5	4.4	5

**Table 2:** Prediction performance of damage estimator for varied debond sizes on one spar at a time.

Cases	Test case 01			Test case 02			Test case 03		
	Spar no.	Debond center	Bolts removed	Spar no.	Debond center	Bolts removed	Spar no.	Debond center	Bolts removed
Target	2	60	31, 32, 33	3	75	31, 32, 33, 34	4	90	31, 32, 33, 34, 35
Prediction	2.1	58.62	2.7	3.2	75.86	3.8	3.3	86.53	4.7

**Table 3:** Neural network performance for load estimation for healthy case with load = 6000 kgs in (a), and 4000 kgs in (b).

(a) Healthy experimental strain data Applied load = 6000 Kgs			(b) Healthy experimental strain data Applied load = 4000 Kgs		
Trial no.	Load predicted (Kgs)	% error	Trial no.	Load predicted (Kgs)	% error
1	5765.8	3.90	1	3723.1	6.92
2	5989.7	0.17	2	4019.8	0.50

**Table 4:** Neural network performance for load estimation; load = 6000 kgs: (a) 1-spar unhealthy case, (b) 2-spar unhealthy case, and (c) 3-spar unhealthy case.

(a) Single spar unhealthy experimental strain data Applied load = 6000 Kgs			(b) Two spar unhealthy experimental strain data Applied load = 6000 Kgs			(c) Three spar unhealthy experimental strain data Applied load = 6000 Kgs		
Trial no.	Load predicted (Kgs)	% variation	Trial no.	Load predicted (Kgs)	% variation	Trial no.	Load predicted (Kgs)	% variation
1	5997.3	0.04	1	6008.1	0.14	1	6135.5	2.26
2	5570.9	7.15	2	6327.2	5.45	2	5230.2	12.83

**6.1.2 Test box 2:** The primary objective of this study was to detect the presence of disbond in such complex, co-cured composite structures. Additionally, the SHM system was expected to estimate the size & location of disbond and predict the load acting on the box. The test box made of Carbon fiber composite, shown in Figure 12(a) and (b), represents a typical wing/empennage structure of a civil aircraft. The box comprises of three spars, a loading rib and two skins. The center spar is co-cured with bottom skin and later secondary bonded to the top skin. A disbond of known size is intentionally created by placing a non-adhesive release film between the top skin and the flange of the mid spar during the lay-up procedure (size 200 mm × 90 mm). Loads were applied to this box and the distributions of strains were measured using several FBG sensors and recorded.

Subsequently, the disbond was partially closed (by 50 mm) using a novel adhesive bonding strategy to reduce its size to 150 mm × 90 mm. After bonding, the bonded area was checked with ultrasonic A-scan to ensure the bond quality followed by the next set of structural tests with this reduced disbond size. Once again, strain data from FBG sensors were acquired and stored. This procedure was repeatedly followed to reduce the size of disbond in steps of 50 mm until the mid-spar and top skin were completely bonded ('healthy box').

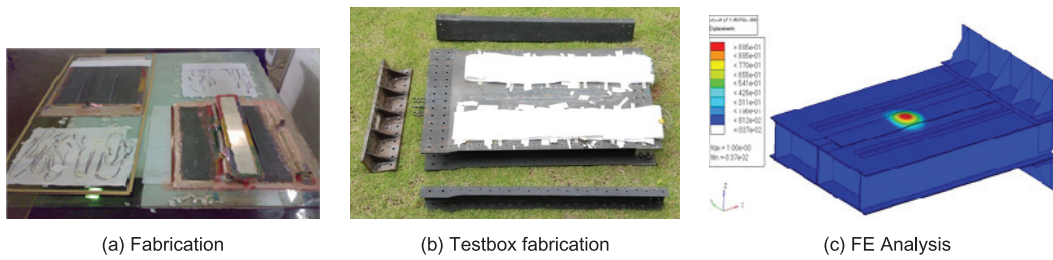
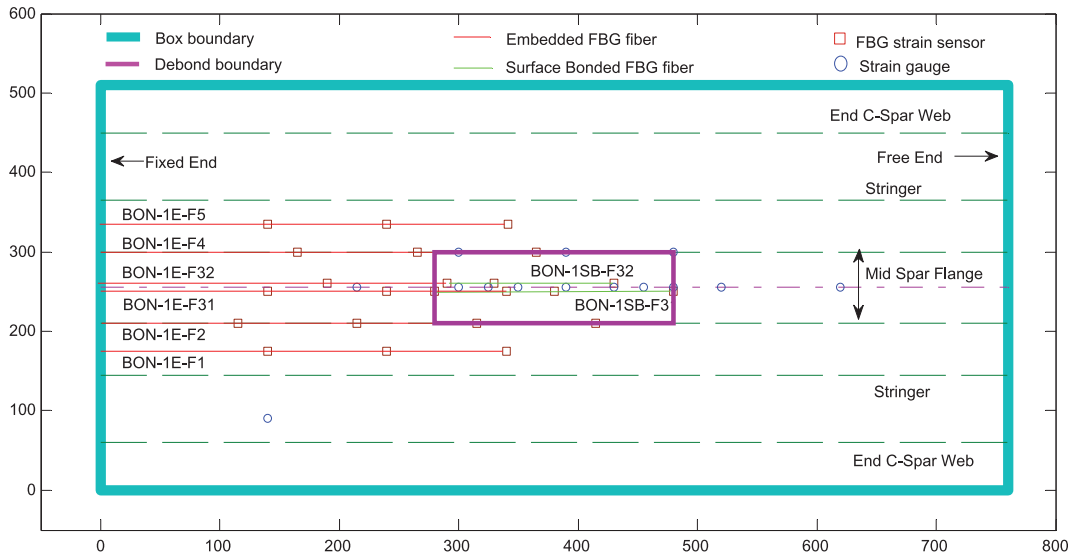
Preliminary finite element analysis was conducted to study the strain distribution and identify the critical strain locations. It was found

from FE analysis that the variation in strain was highest inside the deboned region as shown in Figure 12(c). Figure 13 shows the sensor location diagram. A total of 54 FBG sensors distributed across 18 fibers were embedded in the test box. Additionally 5 FBGs (distributed across two fibers) and 23 Resistance Strain Gauges (SG) were also surface bonded after the assembly of the box.

**6.1.2.1 Experiments:** Three types of loading: i) up bending, ii) down bending iii) bending coupled with torsion, were performed on the test box for each debond size. Details of debond viz., length and location are given in Table 5. The novelty of this study is to vary the length of debond of 200 mm to a smaller debond length in multiple steps, finally leading to a good structure.

Strains measured by FBG sensors and strain gauges show good correlation with FE prediction. Figure 14(a) shows the comparison of the FBG strains with the FE results for different loads for the sensor BON\_1E\_F1\_2. Figure 14(b) shows the comparison of FBG, strain gauge and the FE results for BON\_1E\_F32\_2 sensor. This result is shown for 200 mm debond case.

Figure 15(a) presents the variation in strains on the top skin above mid-spar flange along the span wise direction for 200 mm debond case, loaded under up bending scheme for three different loads of 1200 kg, 2000 kg and 2800 kg. It was seen that even at the load of 1200 kg which is below the buckling load, there was a significant variation in strains inside the debonded


**Figure 12:** Test box used in the study.

**Figure 13:** Sensor location on composite test box.

**Table 5:** Details of debond.

Debond cases	Length (mm)	Width (mm)	Center of debond from the root (mm)
200	200	90	380
150	150	90	355
100	100	90	330

region due to the onset of buckling. At 2000 kg and 2800 kg load, the top skin is into the post-buckling regime. Results from FE analysis display excellent agreement with test data. Figure 15(b) presents the variation in strains on the top skin above mid-spar flange along the span wise direction for the 150 mm debond case and healthy case. The domain of influence of debond was found to be less than 10 mm along the span from the edge of debond. This points to an essential requirement of having at least one sensor within the domain of influence in order to detect the presence of debonds. Good correlation between experimental

and FE strains was observed, thus validating the model developed.

#### 6.1.2.2 Algorithm development and validation:

Two different sets of ANN were implemented in this study. The first set of ANN is concerned with the estimation of expected strain of a malfunctioning FBG, if any.<sup>35</sup> This set of ANN is denoted in the present work as ANN\_MFSE (Malfunctioning Sensor's Strain Estimator). The second set of ANN identifies the state the composite test box. It estimates debond size and location along with the total applied load. This set of ANN is denoted as ANN\_DE (Damage Estimator). Levenberg-Marquardt (L-M)<sup>36</sup> and L-M with Bayesian Regularization<sup>37</sup> was used for the ANN\_MFSE, ANN\_DE respectively.

The ANN\_DE thus implemented was tested against an unseen test case which was not used in training. The test case is taken from experiments performed on the composite test box. The test box contained a debond of size 150 mm × 90 mm located at a distance of 355 mm from fixed end

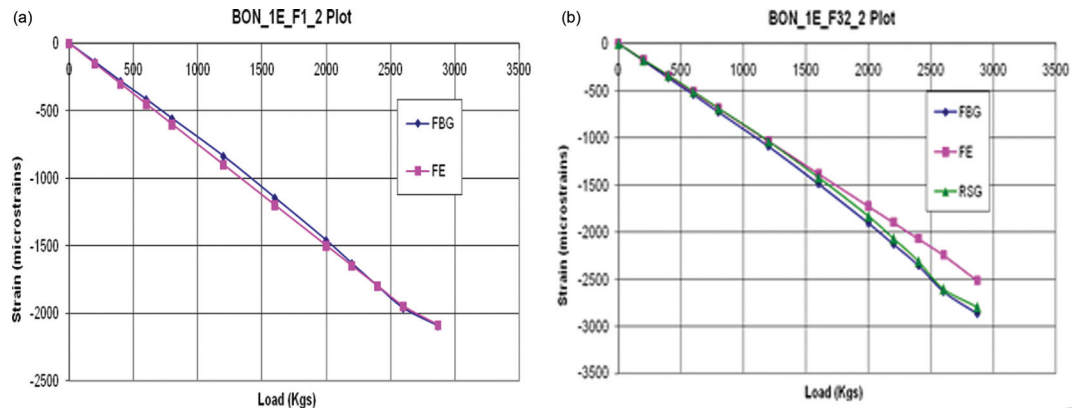


**Figure 14:** (a) Comparison of strains for BON\_1E\_F1\_2 sensor (b) Comparison of strains for BON\_1E\_F32\_2 sensor.

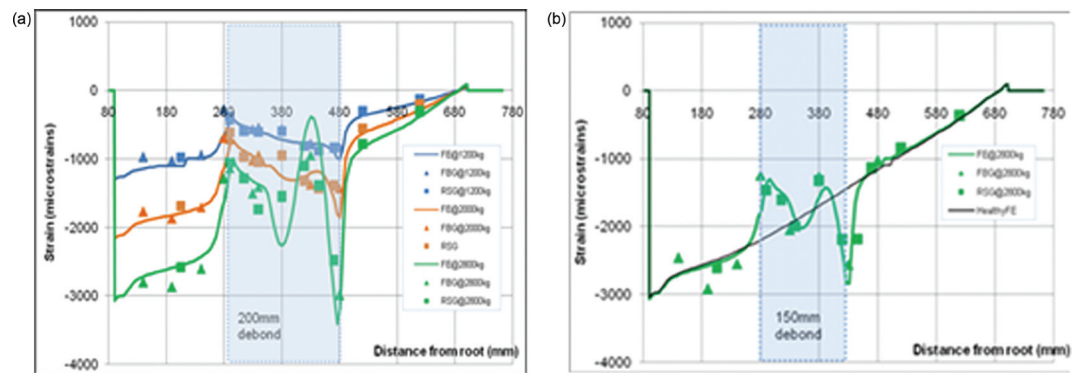


**Figure 15:** (a) Comparison of strains along the span of the box for 200 mm debond up bending cases (b) Comparison of strains along the span of the box for 150 mm debond up bending case.

of the box. Strains captured by the FBG sensors during the experiment formed the input vector for ANN\_DE. The applied load, debond size and debond location estimated by the SHM algorithm are shown in Figures 16(a), 16(b) and 16(c) respectively.

These figures present good agreements between estimated and expected damage parameters and applied load. The RMSE (root mean square error) for total load estimation is 7%, for debond size estimation is 10.6% and for debond location estimation is 2.1%.

Performance of ANN\_MFSE was evaluated based on a test case in which it is assumed that sensor S1 malfunctions and gives zero strains as output. Here two cases were considered. In the first case, the input vector (containing zero strain from malfunctioning sensor) was directly fed to ANN\_DE for estimating load and debond parameters. In the second case, the input vector was first fed to ANN\_MFSE which estimated the expected strain for sensor S1. This estimated strain replaced the zero strain in the input vector and this modified

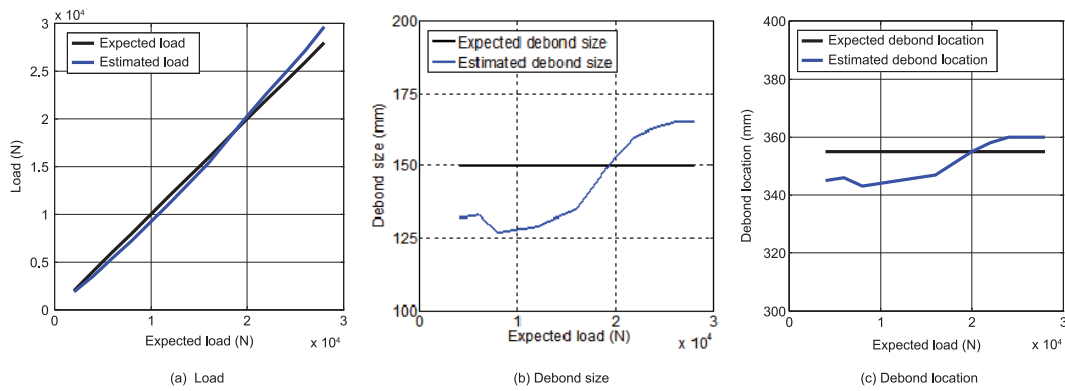
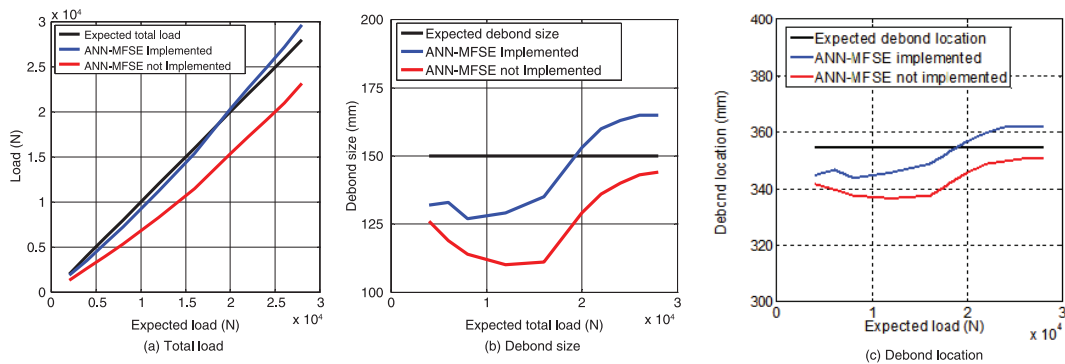
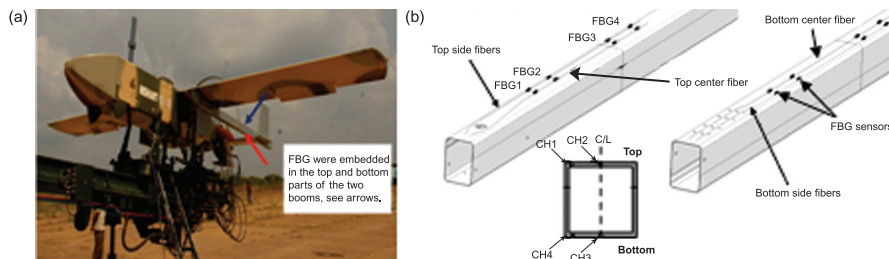
input vector was then fed to ANN\_DE. Comparison of estimations of these two cases along with expected outputs are plotted in Figures 17(a), 17(b) and 17(c).

These results conclude that in case of sensor malfunction, load and debond estimations can be improved appreciably if the process is integrated with ANN\_MFSE.

## 7 Implementation of SHM system and Methods on Unmanned Aircraft

The above mentioned lab level developments were extended to aircraft level as proof of concept. The high maneuverability and harsh operational conditions of modern Unmanned Aerial Vehicles (UAVs), made to select UAV as a platform for this. The overall objective was to demonstrate the operation of an on-board SHM instrumentation under the operating conditions of the Nishant UAV (Figure 18(a)) and determine the operating loads based on the information gathered by embedding fiber optic sensors during the flight. The boom NISHANT UAV was selected

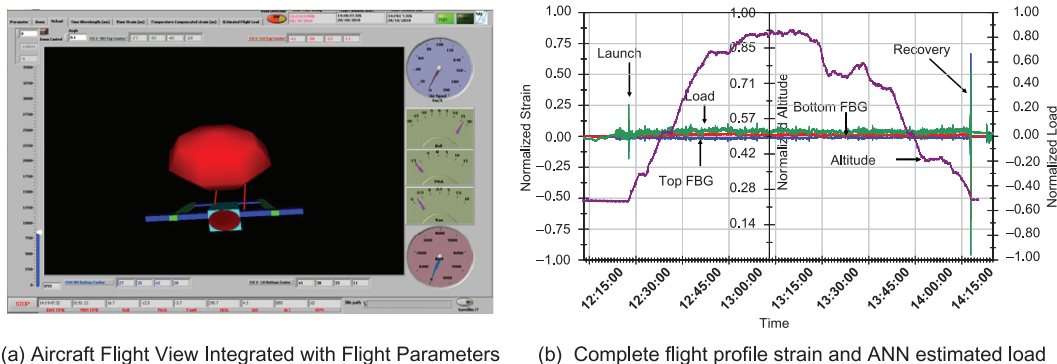



**Figure 16:** Estimation by ANN\_DE.

**Figure 17:** Estimations with and without implementation of ANN\_MFSE.

**Figure 18:** (a) Nishant UAV on launcher (b) Schematic of the boom with FBG embedded.

as the candidate structure which holds hold the tail assembly, comprising a horizontal tail (with elevator) and two vertical tails. In order to track the expected loading conditions, two Fibers were embedded at the centers of the boom and another two Fibers were embedded near the corners Four FBG sensors were imprinted on each Fiber as shown in Figure 18(b).

Patch embedment schemes along with the QA methods were deployed during the embedment during the fabrication stage of the booms.<sup>38</sup> The complete assembly of instrumentation as described in the previous section was placed in the payload bay of the UAV on a specially

designed mounting fixture. These instruments were tested & verified for their functionality, as per the Environmental Screening Specification (ESS) requirements of the UAV.<sup>39</sup> Through necessary static tests ANN based load estimation algorithm was developed and validated on the ground, Flight trial was conducted successfully on 28.10.2010 at Kolar Airfield wherein sensor data were measured online for the entire flight duration of more than two hours. The large size data (>6 GB) collected from the embedded FBG sensors for various flight conditions were processed using LabVIEW based Graphical User Interface (GUI) Flight Data Playback Software QuickVIEW. This software carried



**Figure 19:** QuickVIEW software for flight data processing and processed data.

out temperature compensation to get true structural in-flight strains using Push-Pull Topology, integrated the sensor data with flight parameters such as (engine RPM, altitude, pitch, yaw and roll) to showcase UAV status during various flight events (Figure 19(a)), estimated the operating loads based on the in-flight sensor data using validated ANN based load estimator.<sup>36</sup> Complete flight profile strain and ANN estimated load processed and plotted using the software is shown in Figure 19(b).

## 8 Future Challenges

This is just the beginning of the journey towards realization of a fully online SHM system on an aircraft. The first task towards this goal is to have a system onboard a flying platform to reliably collect sensor data. The next task would be the effective implementation of validated SHM algorithms for the estimation of operational loads. This information will also pave the way for the next paradigm shift to 'SHM Based Design'. The reliable diagnosis of 'significant damage' would be the next challenge, which should be a reality in the next few years. The final challenge is in the prognosis which will give a reliable estimate of the residual life of the structure. This of course is likely to take a much longer time which would necessitate the development of reliable fatigue analysis models.

## Acknowledgements

Thanks are especially due to Mr. B. Ramanaiah & team for carrying out the tests with due diligence. The authors are thankful to Mr. Ramesh Kumar and the NDE group for carrying out the ultrasonic NDE inspection. The authors thank Dr. G.M. Kamath, former Scientist ACD and Mr. M. Subba Rao, former Head ACD for their valuable inputs. Authors also thank the entire staff and students of SHM lab for their diligent work. Authors thank Mr. H.N. Sudheendra, Head,

Advanced Composites Division, for his guidance and support. Authors would also like to express their gratitude to Prof. Moshe Tur, Tel-Aviv University, Mr. Iddo Kressel, IAI, Mr. M. Hariprasad, Dr. A.C.R. Pillai and Mr. G. Natarajan from ADE for their extensive support during the flight trial of SHM system. The unstinted support given by Mr. Shyam Chetty, Director NAL, Dr. A.R. Upadhyya, former Director NAL and Mr. P.S. Krishnan, former Director, ADE is gratefully acknowledged.

Received 1 September 2013.

## References

1. Preeti Pisupati, Sandeep Kumar Dewangan, Dr. Ravi Kumar G.V.V. Feb 2009. Structural Health Monitoring Enabling Technology for paradigm shift in next generation Aircraft. Infosys.
2. Michaels, Kevin. 2008. "MRO 2018: A Glimpse Into The Future." MRO 2008 Conference & Exhibition. Ft Lauderdale.
3. Seth S. Kessler, S. Mark Spearing and Constantinos Soutis. 2001. Structural Health Monitoring in Composite Materials Department of Aeronautics and Astronautics. Technology Laboratory for Advanced Composites.
4. Ramesh Sundaram, G.M. Kamath and Nitesh Gupta. 2012. "Structural Health Monitoring of Composite Structures—Issues and Challenges." *Int. J. Vehicle Structures & Systems* 4(3), 74–85.
5. Roach, D. 2009. "Real time crack detection using mountable comparative vacuum monitoring sensors." *Smart Structures and Systems*. 5(4), pp. 317–328.
6. S.C. Galea, S. Velden, I. Powlesland, Q. Nguyen, P. Ferrarotto, M. Konak, Flight demonstrator of a self-powered SHM system on a composite bonded patch attached to an F/A-18 aileron hinge, in: Asia-Pacific Workshop on Structural Health Monitoring, Yokohama, Japan, 2006.
7. Steven W. Arms, Christopher P. Townsend, Jacob H. Galbreath, Stephen J. DiStasi, Daniel Liebschutz and Nam Phan, "Flight Testing of Wireless sensing Networks

- for Rotorcraft Structural Health and Usage Management Systems” 14 Fourteenth Australian International Aerospace Congress, 7th DSTO International Conference on Health & Usage Monitoring (HUMS 2011).
8. Boller C. 1999. *Adaptronics and Smart Structures systems in aeronautics and space travel*. Heidelberg: Springer-Verlag.
  9. Neidig D., Roach S. 2011. “Does the Maturity of Structural Health Monitoring Technology Match User Readiness.” 8th International Workshop on Structural Health Monitoring. USA: DEStech Publications, Inc. Volume 1.
  10. Balageas, Daniel. 2006. *Structural Health Monitoring*. USA: ISTE Ltd.
  11. Chan T.H.T, Li Z.X. and Ko J.M. 2001. “Fatigue analysis and life prediction of bridges with structural health monitoring data—Part II: Application.” (*International Journal of Fatigue*), 23(1), pp. 55–64.
  12. Coelho C.K., Das S., Chattopadhyay A., Papandreou-Suppappola A. and Peralta P. 2007. “Detection of fatigue cracks and torque loss in bolted joints.” (*Proceedings of SPIE*) 6532 (653204-12).
  13. Hiche C., Liu K.C., Seaver M. and Chattopadhyay A. 2008. “Characterization of impact damage in woven fiber composites using fiber Bragg grating sensing and NDE.” (*Proceedings of SPIE*) 7294 (72940E-11).
  14. Chattopadhyay A., Papandreou-Suppappola A., Peralta P. and Kovvali N. 2010. “A multidisciplinary approach to structural health monitoring and damage prognosis of aerospace hotspots.” (*Aeronautical Journal*) 113(1150), pp. 799–810.
  15. Betz D.C., Thursby G., Culshaw B. and Staszewski W. 2007. “Structural damage location with fiber Bragg grating rosettes and Lamb waves.” (*Structural Health Monitoring*) 6(4), pp. 299–308.
  16. Chang Fu-Kuo. 1999. “Composite structures with built in sensors.” *ICCM 12 Europe*. ICCM.
  17. W.J. Staszewski, S. Mahzan, R. Traynor. 2008. “Health monitoring of aerospace composite structures—Active and passive approach.” (*Composites Science and Technology*).
  18. Kersey A.D. 1992. Multiplexed fibre optic sensors. In: J.E. Pearson (Ed.), 1992, *Optical Technologies for Aerospace Sensing*, Critical Reviews of Optical Science and Technology, Vol. CR47, SPIE, Bellingham, USA, pp. 200–225.
  19. Udd E. (Ed.) (1995). *Fibre Optic Smart Structures*, Wiley Series in Pure and Applied Optics, New York: John Wiley and Sons, Inc.
  20. Measures R. 1992. Advances towards fiber optic based smart structures, *Optical Engineering*, 31(1), p. 35.
  21. Sundaram R., Kamath, G.M., Gupta, N. and Subba Rao, M. (2005). Structural health monitoring of co-cured composite structures using FBG sensors: *Proceedings of the SPIE International Conference on Smart Structures and Systems*, Newport Beach, USA.
  22. Jeannot Frieden, Joël Cugnoni, John Botsis, Thomas Gmür. 2012. “Low energy impact damage monitoring of composites using dynamic strain signals from FBG sensors—Part I: Impact detection and localization.” (*Composite Structures*) 94(2012), pp. 438–445.
  23. Nitesh Gupta, Augustin M.J, Sakthi Sathya, Ramesh Sundaram, M. Hari Prasad, ACR Pillai, S. Gali, J. Balter, P. Gud’s, I. Kressel, A. Hendleman, Y. Botsev, N. Gorbatov, M. Tur (2011) “Flight Data from an Airworthy Structural Health Monitoring System for an Unmanned Air Vehicle Using Integrally Embedded Fiber Optic Sensors” *Proceeding of: International Workshop on Structural Health Monitoring (IWSHM) 2011*, USA: DEStech Publications, Inc.
  24. Doebling C.R. Farrar and S.W. 1999. “Vibration-Based Structural Damage Identification.” *Philosophical Transactions: Mathematical, Physical and Engineering Sciences*, (Royal Society, London).
  25. W.M. West. 1984. “Illustration of the Use of Modal Assurance Criterion to Detect Structural Changes in an Orbiter Test Specimen.” *Air Force Conference on Aircraft Structural Integrity*, pp. 1–6.
  26. S.W. Doebling, C.F. Farrar, M.B. Prime and D.W. Shevits. N.D. “Damage Identification and Health Monitoring of Structural and Mechanical Systems from Changes in their Vibration Characteristics: A Literature Review.” Los Alamos National Laboratory. USA.
  27. T. Inada, Y. Shimamura, A. Todoroki, H. Kobayashi and H. Nakamura. N.D. “Damage Identification Method for Smart Composite Cantilever Beams with Piezoelectric Materials.” *Structural Health Monitoring 2000*. Palo Alto, California, Stanford University.
  28. Xiaomin Deng, Quan Wang, Victor Giurgiutiu. 1999. “Structural health monitoring using active sensors and wavelet transforms.” *SPIE’s 6th Annual International Symposium on Smart Structures and Materials*. Department of Mechanical Engineering.
  29. Shin C.S., et al. 2010. “An FBG-Based Impact Event Detection System for Structural Health Monitoring.” *Advances in Civil Engineering*.
  30. Cristobal Hiche, Clyde K. Coelho and Aditi Chattopadhyay, 2011. “A Strain Amplitude-Based Algorithm for Impact Localization on Composite Laminates.” *Journal of Intelligent Material Systems and Structures*.
  31. K.A. Stevens, R. Ricci and G.A.O. Davies. 1995. “Buckling and postbuckling of composite structures.” *Composites* 26(3), 189–199.
  32. B.G. Falzon, K.A. Stevens and G.A.O. Davies. 2000. “Post-buckling behavior of a blade-stiffened composite panel loaded in uniaxial compression.” *Composites: Part A*, 31, 459–468.
  33. G.M. Kamath, Ramesh Sundaram, Nitesh Gupta and M. Subba Rao, 2010 “Damage Studies in Composite Structures for Structural Health Monitoring using Strain Sensors” *Structural Health Monitoring*, Sage publications doi: 10.1177/1475921710365391.
  34. P. Sakthi Sathya, M.J. Augustin, Gaddikeri Kotresh, Kailash Singh, Ramesh Sundaram “Debond Detection and Load

- Estimation Using Fiber Bragg Grating Sensors on a Composite Test Box—Part I (Experimental Studies)” 6th ISSS International Conference on Microsystems, Smart Materials, Structures [ISSS-2012].
35. Saransh Jain, S.R. Viswamurthy and Nitesh Gupta, P. Sakthi Sathya, M.J. Augustin, Gaddikeri Kotresh, Kailash Singh, Ramesh Sundaram “Debond Detection and Load Estimation Using Fiber Bragg Grating Sensors on a Composite Test Box—Part II (Algorithm Development)” 6th ISSS International Conference on Microsystems, Smart Materials, Structures [ISSS-2012].
  36. Menhaj M.T. Hagan. 1994. “Training feed-forward networks with the Marquardt algorithm.” IEEE Transactions on Neural Networks, 5(6), 1999, pp. 989–993.
  37. D.J.C. MacKay. 1992. “Bayesian interpolation.” Neural Computation, 4(3), pp. 415–447.
  38. Handelman, Y. Botsev, J. Balter, P. Gud’s, I. Kressel, M. Tur, S. Gali, A.C.R. Pillai, M. Hari Prasad, A. Kumar Yadav, Nitesh Gupta, Sakthi Sathya, Ramesh Sundaram, 2010 “Load tracking and structural health monitoring of unmanned aerial vehicles using optical fiber sensors” Proc. SPIE 8173, Photonics 2010: Tenth International Conference on Fiber Optics and Photonics, 81731Z (August 23, 2011); doi: 10.1117/12.898946.
  39. Nitesh Gupta, Augustin M.J, Sakthi Sathya, Ramesh Sundaram, M. Hari Prasad, A.C.R. Pillai, S. Gali, J. Balter, P. Gud’s, I. Kressel, A. Hendleman, Y. Botsev, N. Gorbatov, M. Tur, 2011 “Flight Data from an Airworthy Structural Health Monitoring System for an Unmanned Air Vehicle Using Integrally Embedded Fiber Optic Sensors”, 8th International Workshop on Structural Health Monitoring. USA: DESTech Publications, Inc. Volume 1.



**Mr. Nitesh Gupta** is a Senior Scientist at Advanced Composites Division of CSIR-NAL. His research interest includes Structural Health Monitoring and process monitoring of Composite Structures, Fiber optic sensors and related instrumentation, Signal Processing and Artificial Neural Networks.



**Mr. M.J. Augustin** is project scientist at Advanced Composites Division of CSIR-NAL. His area of interest includes Structural Health Monitoring and process monitoring using Fiber optic sensors, instrumentation, process automation and software implementation in LabVIEW, DIAdem and MATLAB.



**Ms. Sakthi Sathya** is a scientist at Advanced Composites Division of CSIR-NAL. Her research interest includes Design and Finite Element Analysis of composite structures, Structural Health Monitoring, and testing of composite structures.



**Mr. Saransh Jain** is scientist in Advanced Composites Division, CSIR-NAL. His research interests include Design and Development of Composite Structures, Structural Health Monitoring & Damage Tolerance of composites and High velocity (soft body) impact studies.



**Dr. S.R. Viswamurthy** is a Senior Scientist at Advanced Composites Division of CSIR-NAL. His current research interests include: Damage tolerance of composite structures, Structural health monitoring, Computational structural mechanics & Digital image correlation techniques in structural testing. He is a life member of Indian Society for Advancement of Materials and Processing Engineering (ISAMPE).



**Mr. Kotresh M. Gaddikeri** is a principal scientist of the advanced composites division of CSIR-NAL. His research & development interests include (i) Design & development of composite structures (ii) Damage tolerance of composites (iii) Development of 3D composites (iv) Post-buckling of Composites (iv) Digital Image Correlation technique for full field strain measurement.



**Dr. Ramesh Sundaram** is a Senior Principal Scientist and the Deputy head of the Advanced Composites Division of CSIR-NAL. His research interests include Structural Health Monitoring of Composite Structures, Nano Composites, Thermoplastic composites and the like. He is also a member of a number of committees/panels like AR&DB structures panel, AR&DB materials panel, DRDO ‘Vision 2050’ and is also presently the President of ISAMPE.